

Glacier acceleration and thinning after ice shelf collapse in the Larsen B embayment, Antarctica

T. A. Scambos¹, J. A. Bohlander¹, C. A. Shuman², and P. Skvarca³

¹National Snow and Ice Data Center, 1540 30th Street, University of Colorado, Boulder CO 80309-0449, phone 303 492-1113, fax 303 492-2468, email teds@icehouse.colorado.edu

²Oceans and Ice Branch, Code 971, NASA Goddard Space Flight Center, Greenbelt, MD 20771

³División Glaciología, Instituto Antártico Argentino, Cerrito 1248, C1010AAZ, Buenos Aires, Argentina

Abstract. Ice velocities derived from five Landsat 7 images acquired between January 2000 and February 2003 show a two- to six-fold increase in centerline speed of four glaciers flowing into the now-collapsed section of the Larsen B Ice Shelf. Satellite laser altimetry from ICESat indicates the surface of Hektoría Glacier lowered by up to 38 ± 6 m in a six-month period beginning one year after the break-up in March 2002. Smaller elevation losses are observed for Crane and Jorum glaciers over a later 5-month period. Two glaciers south of the collapse area, Flask and Leppard, show little change in speed or elevation. Seasonal variations in speed preceding the large post-collapse velocity increases suggest that both summer melt percolation and changes in the stress field due to shelf removal play a major role in glacier dynamics.

1. Background and Previous Observations

Floating ice shelves are responding rapidly to climate warming in the Antarctic Peninsula. Over the past half-century, mean air temperatures there have increased by 2 to 4°C [King and Comiso, 2003; Skvarca *et al.*, 1999] and in the past 30 years ice shelves in the region have decreased in area by >13,500 km² [Vaughan *et al.*, 1996; Scambos *et al.*, 2003]. In three cases large areas have collapsed suddenly: the Larsen A in January 1995 (1600 km²); Wilkins in March 1998 (1100 km²), and the Larsen B in February-March, 2002 (3200 km²).

Air temperature increases in the 1990s led to longer melt seasons and an increase in melt pond extent on the northernmost ice shelves [Fahnestock *et al.*, 2002]. In the same period, ocean temperatures in the Weddell Sea rose, possibly increasing the rate of basal melting of the Larsen Ice Shelf and thereby contributing to collapse [Shepherd *et al.*, 2003]. However, both Larsen collapse events occurred during record warm air temperatures, when surface melt season length and melt pond extent reached new maxima. Areas with melt ponds disintegrated; adjacent areas with few to none remained. This link between climate warming, melt ponding, and ice shelf collapse prompted the proposal of a melt-enhanced fracture mechanism as the main cause of shelf disintegration [Scambos *et al.*, 2000].

Ice shelf removal has been tied to potential glacier flow increases [Thomas, 1979]. The presence of a shelf provides 'backstress', or longitudinal compressive force, if a mechanical connection exists between the shelf ice and surrounding land areas, ice rises, or islands. However, some models of ice sheet flow show little effect of shelf removal [Hindmarsh, 1996]. The magnitude of this effect is critical to understanding ice sheet mass balance and sea level changes under projected warming conditions.

Melt percolation may also affect the force balance of glaciers. This too has a history in ice mechanics theory [Weertman, 1973], and recent observations have placed the discussion in the context of climate change. Measurements of surface flow speed on ice sheets and glaciers suggest that summer meltwater can descend via crevasses to the bed, seasonally reducing

basal stress and increasing flow speed by up to 25%, even when the glaciers contain ice well below freezing [Zwally *et al.*, 2002a; Boon and Sharp, 2003].

Following the collapse of Larsen A Ice Shelf in January 1995, interferometric synthetic aperture radar (InSAR) revealed that two of its tributary glaciers increased in speed by up to 3-fold [Rott *et al.*, 2002]. The InSAR image pairs were acquired in late 1995 and late 1999. Speed increased throughout the glaciers, but along-flow speed profiles for Drygalski Glacier indicated an abrupt increase in speed gradient in the lowest parts of the glacier trunk. The location of this speed profile 'kink' moved upstream by 8 km in the four-year span. Above the kink, flow speed increased, but more uniformly. The authors note that acceleration may have begun prior to the first survey.

Photographs of the Drygalski Glacier valley walls in early 2002 showed remnant ice ridges ('ice terraces') 20 to 40 m above the glacier surface, indicating a substantial surface lowering [De Angelis and Skvarca, 2003]. Additional satellite image evidence suggested rapid speed increases (surging) for other glaciers flowing into the Larsen A embayment. Here we use speed and elevation data acquired closer in time to a shelf collapse event to study the effects of shelf removal and climate warming on glaciers in more detail.

2. Speed and Elevation Measurements

Five satellite images spanning the period of Larsen B Ice Shelf retreat and collapse are used to map the velocity of six glaciers draining into the Larsen B embayment. Landsat 7 Enhanced Thematic Mapper (ETM+) images from 27 January 2000, 06 December 2001, 06 April 2002, 18 December 2002, and 20 February 2003, were used in an image feature-tracking algorithm [Scambos *et al.*, 1992] to gather ice motion data along selected flow centerline points in the lowest 10 to 12 km of the glaciers. We mapped four glaciers feeding the now-empty northern shelf embayment (Hektoria, Green, Jorum, and Crane) and two glaciers (Flask and Leppard) flowing into the remaining southern ice shelf areas (Figure 1). The images are used in sequential pairs, permitting some seasonal resolution of ice flow variations.

Errors from the image feature-tracking algorithm come from two sources: image mis-registration; and noise in the correlation matches of image 'chip' pairs. For the Larsen B images, mountain ridges allowed co-registration to within a pixel (15 meters for ETM+ band 8). Noise in adjacent correlation matches for the ice motion vectors is approximately 0.25 to 0.5 pixels. The reported centerline values (Figure 1) are averages of 5 to 50 vectors within a

few hundred meters of the selected site. In some cases thin clouds or saturation of the band 8 data forced different approaches, either using unsaturated bands (band 3 and 4 of ETM+) or in one case manually tracking features. Errors shown in the graphs are based on displacement measurement errors of ± 20 meters (1.33 band 8 pixels) to ± 40 meters (where other methods were used).

The first image pair spans summer and winter periods before 2002, so the derived ice motion measurements approximate the average flow speed just prior to ice shelf collapse. The second image pair spans the period of the March 2002 Larsen B shelf collapse, including the warmest summer and most extensive melt season on record at the Matienzo automated weather station (AWS). Mean summer (December-February) air temperature, MST, was $+1.3^\circ$ [Skvarca et al., 2004]. Glacier speed increased by up to 80% for the four northern glaciers, with little variation along the centerlines.

The third sequential image pair covers the winter period following collapse. Glaciers south of the collapse area, Flask and Leppard, show deceleration or no significant change. However, glaciers draining into the collapsed shelf area accelerated significantly, particularly where retreat reached the grounding line prior to the image period, i.e., for Hektor and Green glaciers. Speed gradient in the lower parts of these glaciers also increased greatly. The pattern is amplified in the last image pair, which spans most of the summer of 2003. This summer was much cooler than the previous one (MST -1.2°C), with much less melt, and speed changes for Flask Glacier were small.

At both Jorum and Crane glaciers small sections of shelf ice remained throughout the Landsat image series. For Jorum, the 2002 winter image pair indicates a decrease in flow speed, uniform throughout the lower trunk, though speeds are still greater than the pre-collapse mean. In the last image pair period, both glaciers develop an increased speed gradient in their lower trunk. At this point, the remaining shelf was < 2 km along the centerline for both glaciers.

Longitudinal strain rates at the downstream sites for the Hektor and Green glacier increased from $0.00002\text{--}0.00005\text{ d}^{-1}$ to $0.0003\text{--}0.0008\text{ d}^{-1}$ over the study period. Increased longitudinal extension is also evident in crevasse pattern changes on the glaciers. Figure 2 shows a portion of Hektor Glacier from the third image pair. Crevasse patterns in the earlier image (and the two preceding it) are dominantly fractures associated with left-lateral shear near the east glacier margin. In the later image, the shear pattern is overprinted by dense transverse fracturing. At the southern end of the glacier, chaotic fracturing is

disintegrating the grounded glacier trunk. Airborne visual observations of continued intense fracturing at the glacier terminus in February 2004 by one of us (Skvarca) suggest a continuing increase in glacier speed.

We interpret the speed and acceleration data in Figure 1 to be a combination of at least two patterns: seasonal variations relative to the long-term trend; and a rapid, progressive acceleration of the lowest glacier areas, beginning immediately after ice shelf collapse and progressing upstream. The latter pattern appears to be moderated by even small sections of remaining shelf.

Contours in Figure 3a map the ice speed increase between the two summer Landsat image pairs. Here, the same method used for the centerline areas was applied to the entire lower glacier, resulting in two velocity grids of several hundred vectors. Without continuous velocity measurements it is difficult to completely separate seasonal changes from shelf-loss-related changes, but the presented difference map best isolates the effect of shelf loss on the glacier flow after one year.

Large decreases in glacier surface elevation occurred in the months following collapse. ICESat (Ice, Cloud, and land Elevation Satellite), launched in January of 2003, acquired several elevation profiles across the glaciers beginning shortly after launch. The satellite carries a two-wavelength 40 Hz pulse laser altimeter [Zwally et al., 2002b] that acquires elevation profiles as a series of laser 'shot points' with ground spacing averaging 172 m and effective spot diameters of about 70 m. Elevations reported here are relative to the EGM96 geoid.

Three elevation profiles from an 8-day ICESat repeat track cross Hektor Glacier, two in February and March and the third in September of 2003 (Figure 3a and b). By interpolating elevations between the first two profiles using flow-aligned shot point pairs, we estimate elevations in the location of the later profile. Cloud cover rendered all but 10 shots unusable in the later profile. These 10 elevation values were lower than the interpolated elevations by 5 to 38 meters (and were lower than the February profile located 800 m downstream). We interpret this as an elevation loss due to thinning (averaging 3 to 21 cm d^{-1}) over the span of observations. Slope estimates and elevation changes were iterated twice, to approximate the likely drawdown between the first two profiles. Given the 2002 increase in longitudinal strain rate, implying annual thinning rates of 10 to 25% of the glacier thickness, these 2003 elevation loss rates are consistent with the large scale of the dynamic changes, but may also

indicate a slowing in the rate of acceleration. Glacier thickness is ~300 meters near the grounding line (Scambos et al., 2000).

Under clear sky conditions, ICESat measurements are accurate to ± 20 cm [Zwally et al., 2000b]. Thin cloud cover can cause elevation errors of up to ~2 meters due to scattering in the atmospheric pathway. However, the majority of the error here comes from assuming constant slope between the profiles. We estimate a ± 6 m error based on the average along-track elevation differences from smoothed versions of the two earlier profiles, when filtered at 2.4 km (the spacing between the two outer profiles).

Later acquisitions in a 33-day near-repeat pattern provide coverage of several sections of the other glaciers in late 2003 and early 2004. Repeat track separations are within 200 m, and in all cases the later profiles are to the west (upstream). Figure 4 shows profiles of Crane, Jorum, and lower Flask glacier. The tracks show further shelf disintegration near Crane Glacier in late 2003. Lower Jorum Glacier and upper Crane Glacier profile pairs show average elevation reductions of 3.4 to 4.1 ± 1 m (2.7 to 3.1 cm d^{-1}) after correction for mean along-flow slope. For Flask Glacier, slope-corrected elevations repeat to within 0.2 ± 1 m.

3. Seasonal variations versus post-collapse acceleration characteristics

A large acceleration of the lower portions of the Larsen B glaciers began within months of the collapse of the fronting ice shelf areas. The acceleration, and a dramatic lowering of the glacier surface, progressed upstream over the ensuing months and has continued several years after ice shelf removal. Glaciers south of the shelf collapse area do not show these changes. It appears that a complete removal of the shelf to the grounding line initiates the progressive acceleration.

Seasonal velocity variations before shelf collapse show a different pattern, in which the entire centerline speed profile of the lower glacier alternately increases (summer) and decreases (winter), with little change in longitudinal strain. We attribute this to melt-water percolation to the bed of the glacier, and an ensuing reduction in basal resistance.

Acknowledgments. This work was supported by NASA grant NAG5-11308, and NSF grants OPP-9814550 and OPP-0338134, and Instituto Antártico Argentino.

References

- Boon, S., and M. Sharp, The role of hydrologically-driven ice fracture in drainage system evolution on an Arctic glacier, *Geophys. Res. Lett.* 30 (18), doi:10.1029/2003GL018034, 2003.
- De Angelis, H., and P. Skvarca, Glacier surge after ice shelf collapse, *Science*, 299, (5612) 1560-1562, 2003.
- Fahnestock, M. A., W. Abdalati, and C. Shuman, Long melt seasons on ice shelves of the Antarctic Peninsula: an analysis using satellite-based microwave emission measurements, *Ann. Glaciol.*, 34, 127–133, 2002.
- Hindmarsh, R., Stability of ice rises and uncoupled marine ice sheets, *Ann. Glaciol.*, 23, 105-115, 1996.

- Jezek, K. C., H. Liu, Z Zhao, and B. Li, Improving a digital elevation model of Antarctica using radar remote sensing data and GIS techniques, *Polar Geography* 23,(3), 185-200, 1999.
- King, J. C., and J. C. Comiso, The spatial coherence of interannual temperature trends in the Antarctic Peninsula, *Geophys. Res. Lett.* 30 (2), 1040, doi: 10.1029/2002GL015580, 2003.
- Rack, W., and H. Rott, Pattern of retreat and disintegration of Larsen B ice shelf, Antarctic Peninsula, *Ann. Glaciol.* 39, 2004 (in press).
- Rott, H., W. Rack, P. Skvarca, and H. De Angelis, Northern Larsen Ice Shelf, Antarctica: further retreat after collapse, *Ann. Glaciol.*, 34, 277-282, 2002.
- Scambos, T., M. Dukiewicz, J. Wilson, and R. Bindshadler, Application of image cross-correlation to the measurement of glacier velocity using satellite image data, *Remt. Sens. Environ.*, 42 (3), 177-186, 1992.
- Scambos, T., C. Hulbe, M. Fahnestock, and J. Bohlander, The link between climate warming and break-up of ice shelves in the Antarctic Peninsula. *J. Glaciol.*, 46 (154), 516-530, 2000.
- Scambos, T., C. Hulbe, and M. Fahnestock, Climate-induced ice shelf disintegration in the Antarctic Peninsula, in *Antarctic Peninsula Climate Variability; historical and paleoenvironmental perspectives*, edited by E. Domack and five others, pp. 79-92, AGU, Washington, D.C., 2003.
- Shepherd, A., D. Wingham, T. Payne, and P. Skvarca, Larsen ice shelf has progressively thinned, *Science* 302 (5646), 856-859, 2003.
- Skvarca, P., W. Rack, H. Rott, and T. Ibarzábal y Donánglo, Climatic trend, retreat and disintegration of ice shelves on the Antarctic Peninsula: an overview, *Polar Research* 18 (2), 151-157, 1999.
- Skvarca, P., H. De Angelis, and A. Zakrajsek, Climatic conditions, mass-balance, and dynamics of Larsen B Ice Shelf, Antarctic Peninsula, prior to collapse, *Ann. Glaciol.* 39, 2004 (in press).
- Thomas, R. H., T. O. Sanders, and K. E. Rose, Effect of warming on the West Antarctic Ice Sheet, *Nature*, 277 (5695), 355-358, 1979.
- Vaughan, D. G., and C. S. M. Doake, Recent atmospheric warming and retreat of ice shelves on the Antarctic Peninsula. *Nature*, 379, 328-331, 1996.
- Weertman, J., Can a water-filled crevasse reach the bottom surface of a glacier?, *Int. Assoc. of Scientific. Hydrology Publication*, 95, 139-145, 1973.

- Zwally, H. J. , W. Abdalati, T. Herring, K. Larson, J. Saba, and K. Steffen, Surface melt-induced acceleration of Greenland ice-sheet flow, *Science*, 297 (5579), 218–222, 2002a.
- Zwally, H. J., R. Shutz, W. Abdalati, and six others, ICESat's laser measurements of polar ice, atmosphere, ocean, and land, *J. Geodynamics*, 34 (3-4), 405–445, 2002b.

FIGURE CAPTIONS

Figure 1. Center panel: MODIS image from 1 November 2003 of the study area with April ice shelf extents and the grounding line (black; Rack and Rott, 2004) for the Larsen B Ice Shelf between 1998 and 2002. Red boxes are speed measurement sites along lower glacier centerlines. Short blue lines indicate locations of ICESat laser altimetry ground tracks over glacier trunks. Surrounding graphs: centerline ice speeds and downstream site accelerations for six glaciers. Landsat 7 image acquisition dates are shown as triangles on the *x*-axes. Grey bars represent the Feb.-Mar. 2002 shelf collapse event.

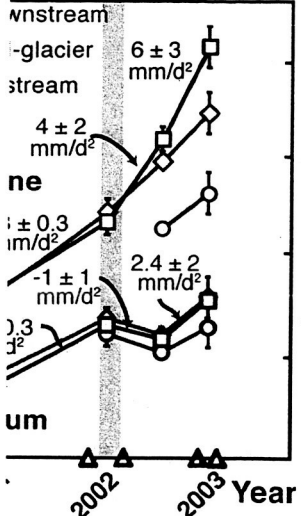
Figure 2. Landsat 7 subscenes showing crevasse changes in the lower Hektor Glacier. Image area is 6 km by 6 km, north is up.

Figure 3, a and b. a: Landsat 7 image from 20 February 2003, with shot point locations from three ICESat tracks overlain. Contours are ice speed *difference* in meters per day between the periods 06 December 2001 – 06 April 2002 and 18 December 2002 – 20 February 2003. Valid elevation locations are shown as red dots. Blue bars connect three elevations along a flow line. Net elevation difference relative to our estimate is shown as text.

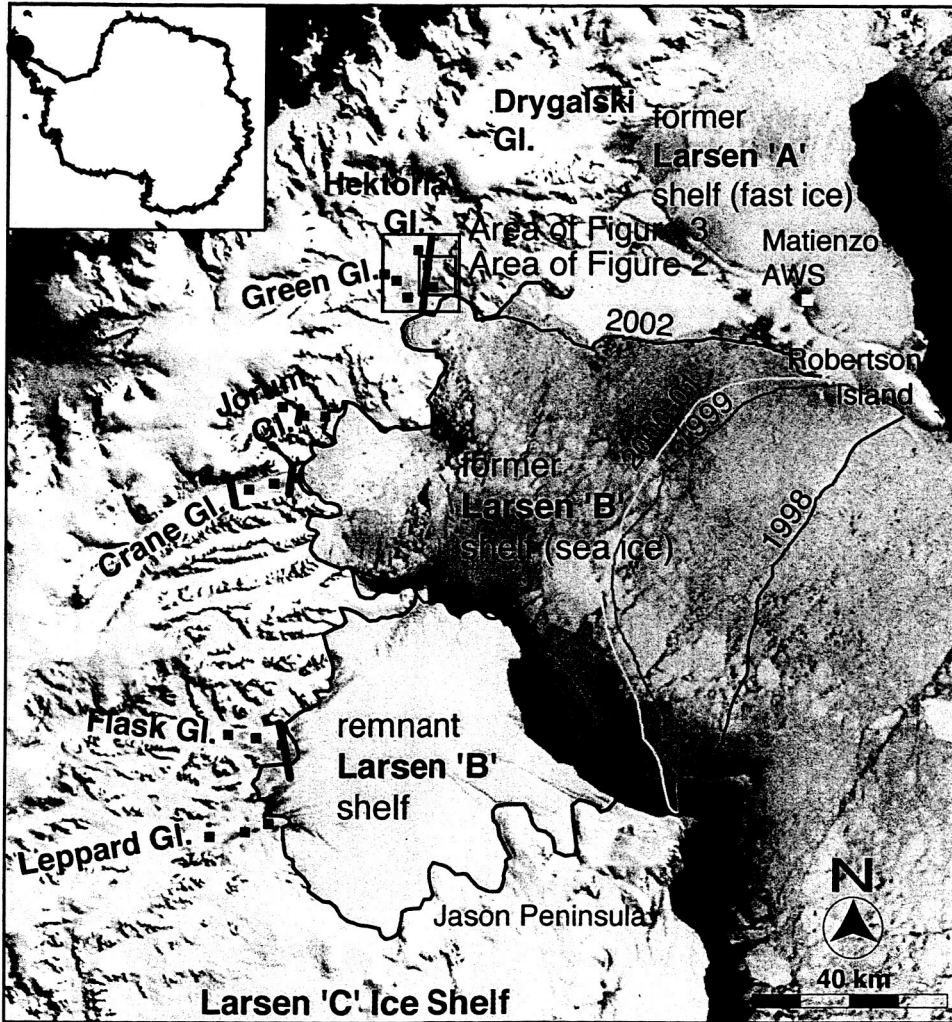
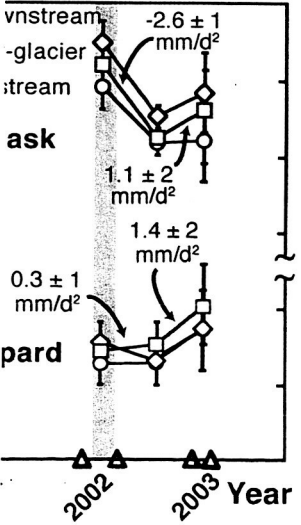
b: ICESat elevation profiles projected up-flow. Red circles are sized to the estimated elevation error of ± 6 m.

Figure 4. ICESat elevation profiles of Jorum, Crane, and Flask glaciers. All profiles looking up-glacier. Mean along-flow slopes of the lower 10 km of the glaciers were determined from Jezek et al. [1999], and used to adjust the net elevation changes.

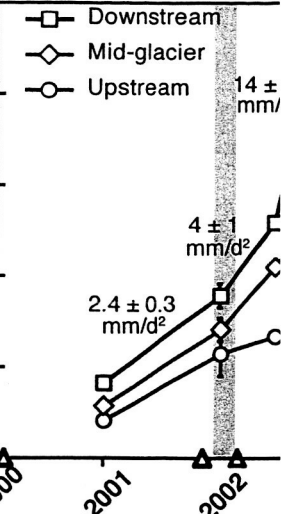
And Jorum Glacier



And Leppard Glacier



Hektoria Glacier



Green Glacier

